

inant factor in the relaxation of the amorphous domains, then the faster relaxing domains reflect an increased proton density and could be compared to a dispersed rubbery phase within more rigid domains. Their presence, not surprisingly, seems to favor improved impact properties. If one disregards the biexponential decay of the amorphous peak and concentrates only on the average value of  $T_{1\rho}(\text{H})$ , this conclusion is not so obvious for the PE1 composites but still valid for the PE2 composite series.

The analysis of just a few samples is not enough to confirm these suggestions or to determine which is the decisive factor: the presence of monoclinic crystals, the differences in amorphous relaxation, or both. But the initial results definitely warrant a more systematic study of the correlations of  $T_{1\rho}(\text{H})$  values in various PE samples with some of the mechanical properties. Filler content and processing parameters will have to be varied, and their effect on the  $T_{1\rho}(\text{H})$  will have to be quantified. Indirect results could be obtained on the phase structure of the PE

components in its composites.

The results presented here also show that  $T_{1\rho}(\text{H})$  is a parameter which may offer valuable information in multicomponent materials. Its use as a probe for blend miscibility is well established. It also gives information on nonbonding interactions, interfacial communication,<sup>13</sup> and, as demonstrated here, on formation of different amorphous domains in polyethylene composites under different processing procedures.

**Acknowledgment.** The contributions of Dr. Graham White and the research team at Du Pont Canada in the form of samples and helpful discussions are gratefully acknowledged. Also appreciated is the spectrometer time offered by Du Pont Canada for running these experiments. Partial financial assistance from NSERC Canada is acknowledged as well.

**Registry No.** Polyethylene, 9002-88-4; calcium carbonate, 471-34-1; cellulose, 9004-34-6.

## Influence of Oxygen on the Stability of $\text{Zr}_4\text{Sn}$

Young-Uk Kwon and John D. Corbett\*

Department of Chemistry and Ames Laboratory—DOE,<sup>1</sup> Iowa State University, Ames, Iowa 50011

Received August 12, 1991. Revised Manuscript Received November 12, 1991

Contradictions regarding the stability of  $\text{Zr}_4\text{Sn}$  have been resolved in terms of the effects of oxygen (and perhaps other) impurities. The phase is stable at 800–1050 °C (at least) and has the composition  $\text{Zr}_{4.0-4.2}\text{Sn}$ , but the decomposition  $3\text{Zr}_4\text{Sn} \xrightarrow{\text{O}_2} \alpha\text{-Zr}(\text{Sn},\text{O}) + \text{Zr}_5\text{Sn}_3$  is driven by the solution of oxygen in the metal. Even trace amounts give three-phase products, such as on the surface of substantially all arc-melted and annealed samples of  $\text{Zr}_4\text{Sn}$ , and the decomposition is complete at 1050 °C in the presence of  $\geq 3$  at. % oxygen. The separate and combined effects of tin and oxygen solutes on the lattice constants of  $\alpha\text{-Zr}$  support the conclusions. The effect of oxygen (Fe, etc.) impurities on the solidus composition for  $\alpha\text{-Zr}(\text{Sn})\text{-Zr}_4\text{Sn}$  may be responsible for some literature differences.

### Introduction

During a recent study of the  $\text{Zr}_5\text{Sn}_3\text{-Zr}_5\text{Sn}_4$  portion of the Zr–Sn system, our interest was also drawn to the  $\text{Zr}_4\text{Sn}$  region.<sup>2</sup> Reports on this phase have been contradictory as regards its composition, structure, and stability. Our investigations at that time supported the conclusion of a critical evaluation of the literature,<sup>3</sup> that the composition is near  $\text{Zr}_4\text{Sn}$  (as originally assigned<sup>4</sup>), and that the structure is the cubic A15 ( $\text{Cr}_3\text{Si}$ ) type. The compound appears to be a line phase at 1000 °C judging from its lattice constants. Other assignments of a  $\text{Zr}_3\text{Sn}$  composition<sup>5-7</sup> were evidently only nominal and based on the structure type. However, our studies also showed that additional, very weak diffraction lines were regularly observed in the

Guinier powder pattern of  $\text{Zr}_4\text{Sn}$  that required a doubling of the unit cell ( $a = 11.252 \text{ \AA}$ ). Although the responsible superstructure has not been established, a predominantly substitutional ordering of the excess zirconium seems probable.

The stability properties of  $\text{Zr}_4\text{Sn}$  are more problematical. Some investigators have reported that  $\text{Zr}_4\text{Sn}$  is stable only at high temperatures,<sup>6,8,9</sup> while one early study did not find this compound at all.<sup>10</sup> A marginal stability has been suggested.<sup>3</sup> Our earlier work<sup>2</sup> indicated that complete conversion to  $\text{Zr}_4\text{Sn}$  was difficult to achieve, and some partial decomposition seemed to occur on equilibration at 820 °C. Although  $\text{Zr}(\text{Fe},\text{Ni},\text{Cr})_2$  compounds have been well identified as precipitates in zircalloys ( $\sim 98\% \text{ Zr}$ , 1.2–1.7% Sn, 0.2–0.5% Fe, Ni, Cr, ...), the precipitation of  $\text{Zr}_4\text{Sn}$  from these alloys has never been seen<sup>11-14</sup> even though the ac-

(1) The Ames Laboratory—DOE is operated for the U.S. Department of Energy by Iowa State University under Contract No. W-7405-Eng-82. This research was supported by the Office of Basic Energy Sciences, Materials Sciences Division.

(2) Kwon, Y.-U.; Corbett, J. D. *Chem. Mater.* 1990, 2, 27.

(3) Abriata, J. P.; Bolcich, J. C.; Arias, D. *Bull. Alloy Phase Diagrams* 1983, 4, 147.

(4) McPherson, D. J.; Hansen, M. *Trans. Am. Soc. Met.* 1953, 45, 915.

(5) Gran, G.; Andersson, S. *Acta Chem. Scand.* 1960, 14, 956.

(6) Rossteutscher, W.; Schubert, K. *Z. Metallkd.* 1965, 56, 815.

(7) Naik, U.; Banerjee, S. *Trans. Indian Inst. Met.* 1978, 31, 318.

(8) Schubert, K.; Anantharaman, T. R.; Ata, H. O. K.; Meissner, H. G.; Pötzschke, M.; Rossteutscher, W.; Stolz, E. *Naturwissenschaften* 1960, 47, 512.

(9) Luo, H. L.; Vielhaber, E.; Corenzwit, E. *Z. Phys.* 1970, 230, 443.

(10) Nowotny, H.; Schachner, H. *Monatsh. Chem.* 1953, 84, 169.

(11) Speich, G. R.; Kulin, S. A. *Zirconium and Zirconium Alloys*; American Society of Metals: Metals Park, OH, 1953; p 200.

(12) Vander Sande, J. B.; Bement, A. L. *J. Nucl. Mater.* 1974, 52, 115.

(13) Vitikainen, E.; Nenonen, P. *J. Nucl. Mater.* 1978, 78, 362.

cepted Zr-Sn phase diagram<sup>3</sup> would lead to this expectation. Studies on the aging of zirconium-tin alloys containing 1.2–6.6 at. % Sn by Carpenter et al.<sup>15</sup> were especially puzzling since little or no precipitation of Zr<sub>4</sub>Sn, or any other phase, was observed. The volume fraction of a second phase, tin-richer but too small to analyze, was in all cases  $\leq 1\%$  and unaffected by aging according to SEM and TEM studies, in contradiction to 20–30% Zr<sub>4</sub>Sn as a second phase predicted by the phase diagrams then available.<sup>4,11</sup> One tentative explanation was that decomposition of Zr<sub>4</sub>Sn might have taken place with precipitation of the next phase, Zr<sub>5</sub>Sn<sub>3</sub>.

Our initial plan for the present study was to clarify the stability or instability of Zr<sub>4</sub>Sn in the (nominal) binary system at  $\sim 800$ – $1050$  °C. Our intuition was that some unrecognized chemistry was probably involved, particularly as little attention had been paid to the effects of potential impurity elements. The research in fact established a dominant role of oxygen in the stability property. This and literature data suggest that such effects may also play an important role in determinations of the neighboring  $\alpha$ -Zr(Sn) solidus boundary.

### Experimental Section

**Materials.** All powdered reactants and products were handled only in a glovebox (Vacuum Atmospheres) in which O<sub>2</sub> and H<sub>2</sub>O were continuously removed from the He atmosphere. The gas routinely contained  $\leq 0.1$  ppm (vol) H<sub>2</sub>O. Pressing of pellets prior to sintering and sample mounting for Guinier powder diffraction were both carried out within the box.

The zirconium metal used in all experiments was reactor-grade crystal-bar material that had principal impurities, in ppm atomic, of Fe 680, Ni 350, Hf 100 (by spark source mass spectrometry) and O 220, C 190 (by vacuum fusion). The metal was cold-rolled to sheet, cut into strips, and cleaned (45:10:45 HNO<sub>3</sub>:HF:H<sub>2</sub>O). Powdered zirconium was again<sup>2</sup> produced through a sequence of hydrogenation, grinding, and dehydrogenation treatments, the last at 700 °C in high vacuum until gas evolution effectively ceased. The lattice parameters of the metal thus obtained matched the literature values for  $\alpha$ -Zr<sup>16</sup> well. No dross was evident on fusion of the tin employed (Baker's analyzed: 99.99%), meaning that nonmetal impurities were at a low level. Since ZrSn<sub>2</sub> can be easily ground to a powder prior to sintering reactions, this was synthesized as a reactant by allowing stoichiometric amounts of tin and zirconium powder to react in a welded<sup>17</sup> Ta tube at 800 °C. The lattice symmetry and dimensions (TiSi<sub>2</sub> type, *Fddd*, *a* = 9.577 (1) Å, *b* = 5.6434 (6) Å, *c* = 9.9287 (9) Å) matched the literature data<sup>10</sup> for ZrSn<sub>2</sub>. ZrO<sub>0.1</sub> chips were synthesized by allowing the metal to react with a measured amount of oxygen. The lattice parameters of the product agreed well with those reported for that composition.<sup>16,18</sup>

**Syntheses.** Arc melting in a Centorr 5SA arc furnace followed by annealing reactions were employed in many cases. In the most careful work, the arc was held on a zirconium getter for at least 20 s immediately before and after each sample was melted in order to reduce contamination from impurities in the argon atmosphere. The effect of such an operation was obvious as the product buttons had much shinier surfaces. These were turned over and so remelted at least three times in an effort to ensure homogeneity. The product weights were compared with those of the starting reagents in order to correct for tin losses during melting; however, these were negligible in most cases. The necessary annealings, typically 1000 °C for 7 days, were subsequently carried out in sealed Ta containers that were in turn sealed within well-evacuated, baked silica jackets. A liner of 0.003-in. molybdenum sheet in the Ta container was found to be effective in eliminating loss

of zirconium from Zr-rich alloys into the Ta that otherwise occurs at  $\sim 1000$  °C or above. The metal container system is much preferred over sealed fused silica alone where contamination problems originate from the inevitable H<sub>2</sub>O that evolves therefrom during the reactions, especially if the silica is not strongly heated first. (Some passage of water effectively through Ta tubing probably occurs anyway.) Silica will also vapor phase transport in the presence of H<sub>2</sub> (from H<sub>2</sub>O) near or above 1000 °C, and this is prevented by the intervening Ta.

Reactive sintering reactions were also carried out to produce some Zr<sub>4</sub>SnO<sub>y</sub> samples (0.5).<sup>19</sup> stoichiometric amounts of powdered Zr, ZrSn<sub>2</sub>, and Zr<sub>5</sub>Sn<sub>3</sub>O<sub>x</sub> (*x* = 0.1 or 0.5).<sup>19</sup> The ternary oxide reactant served as a deliberate oxygen source and had been previously prepared by arc melting suitable proportions of Zr, Sn, and ZrO<sub>0.1</sub> followed by grinding of the button. Both annealing and sintering reaction containers were quenched in water.

**X-ray Diffraction.** Guinier powder X-ray diffraction was utilized to provide estimates of the yields of phases as well as to obtain accurate lattice parameters. NBS (NIST) silicon was added to the samples as an internal calibrant. The relative diffraction intensities of different phases in a sample were used as rough measures of their relative proportions.

**SEM Studies.** A JEOL JSM-840 scanning electron microscope with a KEVEX EDX system was employed in the distribution and compositional study of some samples.

### Results and Discussion

Synthesis means for Zr<sub>4</sub>Sn reflect the phase relationships first outlined by McPherson and Hansen.<sup>4</sup> Its composition is very close to that of the  $\beta$ -Zr-Zr<sub>5</sub>Sn<sub>3</sub> eutectic that forms at  $\sim 1592$  °C following arc melting. Annealing this product below the 1327 ( $\pm 20$ ) °C peritectoid is necessary to produce Zr<sub>4</sub>Sn, while the adjoining  $\beta$ -Zr(Sn), if any, transforms to  $\alpha$ -Zr(Sn) at 982 °C. SEM-EDX analyses of the phase in annealed samples of bulk composition Zr<sub>4+x</sub>Sn,  $-0.20 \leq x \leq 0.61$ , gave Zr:Sn ratios of 4.00:1 to 4.24:1 ( $\pm 0.15$ :1 in each).

The thought that the Zr<sub>4</sub>Sn decomposition observed earlier might follow from the  $\beta \rightarrow \alpha$  zirconium transformation was easily disproven; annealing Zr<sub>4</sub>Sn pellets above or below this point did not make any difference. On the other hand, our best Zr<sub>4+x</sub>Sn products were puzzling as the powder patterns for those with *x*  $\leq 0.1$  (including negative values) always showed both of the adjoining phases  $\alpha$ -Zr and Zr<sub>5</sub>Sn<sub>3</sub>, even though each usually gave less than 5% of the diffraction intensity of the major Zr<sub>4</sub>Sn (for small *x*), and the zirconium lines were often diffuse and weak. This result was reproducible, regardless of the annealing temperature or reaction time, typically 950–1000 °C or higher and 7 days or longer, respectively. On the other hand, annealed samples with *x*  $\geq 0.2$  showed only Zr<sub>4</sub>Sn and  $\alpha$ -Zr(Sn).

Even though three phases were always seen in the powder patterns of the former group (*x*  $\leq 0.1$ ), the possibility of an incomplete equilibration could not immediately be ruled out. To enhance diffusion and the attainment of equilibria, some annealed buttons were ground to fine powders, pressed into pellets, and sintered at 900–1000 °C for 7 days or longer. Such treatments of Zr<sub>5</sub>Sn<sub>3+x</sub> ( $0 \leq x \leq 1$ ) compositions were earlier<sup>2</sup> found to have a dramatic effect on equilibration rates; as-casts in this range have large Zr<sub>5</sub>Sn<sub>3+x</sub> crystal domains and gross composition inhomogeneities associated with the particular phase relationships, and these could effectively be eliminated by only mechanical means. Crystallites were evident by SEM in as-cast and annealed Zr<sub>4</sub>Sn, although the phase relationships are quite different. However, such a grinding-sintering procedure gave no evident reduction of the minor phases; in fact, the powder patterns of the sup-

(14) Versaci, R. A.; Ipohorski, M. *J. Nucl. Mater.* 1979, 80, 180.

(15) Carpenter, G. J. C.; Ibrahim, E. F.; Watters, J. F. *J. Nucl. Mater.* 1981, 102, 280.

(16) Holmberg, B.; Dagerhamn, T. *Acta Crystallogr.* 1961, 15, 919.

(17) Corbett, J. D. *Inorg. Synth.* 1983, 22, 15.

(18) Seaverson, L. M.; Corbett, J. D. *Inorg. Chem.* 1983, 22, 3202.

(19) Kwon, Y.-U.; Corbett, J. D., to be submitted for publication.

Table I. Phases Present in  $Zr_4SnO_y$  Compositions

$y$	at. % O	synthesis conditions <sup>a</sup>	phases present <sup>b</sup>	Zr lattice parameters		
				$a$ , Å	$c$ , Å	$c/a$
0.033	0.66	S <sup>c</sup>	$\alpha$ -Zr, $Zr_4Sn$ , $Zr_5Sn_3$			
0.10	2.0	AA	$\alpha$ -Zr, $Zr_4Sn$ , $Zr_5Sn_3$	3.2214 (8)	5.162 (3)	1.602
0.15	2.9	AA	$\alpha$ -Zr, $Zr_4Sn$ , $Zr_5Sn_3$			
0.17	3.2	S <sup>c</sup>	$\alpha$ -Zr, $Zr_5Sn_3$			
0.20	3.8	AA	$\alpha$ -Zr, $Zr_5Sn_3$			
0.40	7.4	AA	$\alpha$ -Zr, $Zr_5Sn_3$	3.2411 (3)	5.1705 (4)	1.5953

<sup>a</sup>S: sintered Zr and  $Zr_5Sn_3O_x$  powders, 1050 °C, 7 days. AA: arc-melted Zr,  $ZrO_{0.1}$ , Sn annealed at 1050 °C for 7 days and quenched.  
<sup>b</sup>From Guinier powder diffraction. <sup>c</sup>Incomplete reaction, as expected.

posedly better equilibrated samples always showed some increased intensities for the two extra phases.

The spontaneous decomposition of the binary phase that is implied by the instability suggested by some authors is not correct. Sintering of powders of Zr and either  $Zr_5Sn_3$  or  $ZrSn_2$  in proportions to give  $Zr_4Sn$  at 800 or 1000 °C for 7–14 days also provided  $Zr_4Sn$ , Zr, and  $Zr_5Sn_3$  but with a lower proportion of  $Zr_4Sn$ . Different intensity distributions among the three phases in the latter samples under different conditions indicated that the systems were far from equilibria and suggested that the driving force was small. Nonetheless, since  $Zr_4Sn$  did form, an instability or metastability at 800–1000 °C is not germane.

The fact that substantially all samples of  $Zr_4Sn$  prepared by arc melting and annealing that were on-stoichiometry or slightly tin-rich also contained  $\alpha$ -Zr(Sn) and  $Zr_5Sn_3$  must mean that we were actually dealing with a three-phase system. Others have seemingly encountered the same three-phase synthesis result.<sup>4,6</sup> The prevalence of oxygen as an impurity led us to postulate that this was the cause under substantially all arc-melting and sintering conditions, even with the best materials. Accordingly, various amounts of oxygen were deliberately added to  $Zr_4Sn$  compositions in melt-anneal or sinter reactions, and these provided the results summarized in Table I.

The same three phases,  $\alpha$ -Zr,  $Zr_4Sn$ , and  $Zr_5Sn_3$ , were observed in quenched  $Zr_4SnO_y$  products up through  $y = 0.15$ , whereas only two phases,  $\alpha$ -Zr and  $Zr_5Sn_3$ , were found in oxygen-richer samples, viz.,  $y = 0.17$  by sintering and  $y = 0.20, 0.40$  by melt-anneal. Although the former sintered sample was clearly not at equilibrium, it is still significant that  $Zr_4Sn$  was evidently not obtained at the ~5% detection limit. Clearly  $Zr_4Sn$  is extremely sensitive to oxygen, to the point that it is completely decomposed at 1050 °C by more than about 3 at. % oxygen. Even in the oxygen-poorer samples, the  $Zr_4Sn$  showed the lesser diffraction intensities, e.g., 20–30% at  $y = 0.1$  (2 at. % O). These results also provide a plausible explanation for the absence of  $Zr_4Sn$  in an early study of the Zr–Sn system since the metal used contained ~2.4 wt. % oxygen.<sup>10</sup> The amount of impurity oxygen in our “best” binary samples prepared by arc melting–annealing procedures must have been extremely small and perhaps beyond control under conventional conditions, since only a 90–95% yield of  $Zr_4Sn$ ,  $\alpha$ -Zr(Sn,O) and  $Zr_5Sn_3$  making up the rest, was indicated by the relative diffraction intensities.

The powder pattern line positions and the lattice constants calculated therefrom for the  $Zr_4Sn$  and  $Zr_5Sn_3$  components in these samples did not change with oxygen

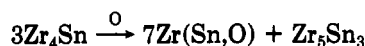
content. This indicates the oxygen is partitioned entirely into the zirconium. Estimation of the oxygen content based on lattice parameters is not possible since the metal system is now ternary  $\alpha$ -Zr(Sn,O), for which there are no data. Lattice parameters for  $\alpha$ -Zr(O)<sup>16,18</sup> and  $\alpha$ -Zr(Sn)<sup>11,20</sup> as a function of solute concentration show contrasting behaviors in the dilute region. The value of  $a$  increases with oxygen content but decreases with tin, while the  $c$  parameters increase with both, somewhat more rapidly with tin, so that trends in  $c/a$  for the two cases are quite distinctive. The lattice dimensions of the metal phase in the  $y = 0.4$  sample, Table I, clearly show more Zr(O) character while those for  $y = 0.1$  look more like Zr(Sn). These elements may not necessarily compete with each other in  $\alpha$ -Zr in the dilute composition region since tin reportedly dissolves substitutionally while oxygen occurs in interstitial sites. The lattice constants of the 10–20% zirconium phase present on one  $Zr_4Sn$  sample ( $a = 3.2185$  (4),  $c = 5.1542$  (6) Å) are clearly not those of  $\alpha$ -Zr(Sn) or  $\alpha$ -Zr(O) but are consistent with a mixture of solutes.

The question as to the sample preparation stage in which most of the impurity oxygen was introduced had three reasonable answers: the arc-melting process, during annealing, or during exposure of the sample to air after arc melting. The third possibility was easily eliminated with a  $Zr_4Sn$  sample that had been arc-melted, annealed, and powdered. Separate portions were stored in air and in the glovebox for 100 h, much longer than usual, and these then separately pelleted and sintered. The powder patterns of the two products were indistinguishable in both the line positions and the intensity distributions for all phases. However, this may not completely exclude contamination during storage in air for long periods of time, particularly with as-cast samples because the  $Zr_5Sn_3$  component in these is the most moisture-sensitive phase in the system. We suspect that the previously reported signs of decomposition of  $Zr_4Sn$  upon annealing at 820 °C<sup>2</sup> arose from contamination during exposure of the pellet to air for months before annealing.

To better judge the arc-melting process, the outer surface of a normal (shiny) as-cast sample of  $Zr_4Sn$  composition was filed off in air, and the remaining sample annealed, ground, pressed into a pellet, and sintered as before. The powder pattern of this contained weak lines of  $\alpha$ -Zr and  $Zr_5Sn_3$  but their intensities were less than half of those found otherwise. Furthermore, the powder pattern of the surface filings showed mainly Zr and  $Zr_5Sn_3$ . Therefore, we conclude that the oxygen impurity must have been introduced principally during the arc-melting process and, since the button solidified within seconds after the arc was turned off, the oxygen was more concentrated on the surface. However, sintering a ground pellet from a melt-anneal process nearly always resulted in an observable increase in Zr and  $Zr_5Sn_3$  components in the X-ray pattern. Some of this may reflect the selection process for a powder pattern, which may not adequately sample the pellet surface after the melting step. In addition, some traces of oxygen can be introduced during the sintering and annealing processes, most likely from traces of water evolved from the  $SiO_2$  jacket that can permeate the tantalum container at these temperatures.

There is a special character to the decomposition experiments typified by the results in Table I since the compositions were aimed at pure  $Zr_4Sn$ . Since oxygen does not have a significant solubility in  $Zr_4Sn$ , or in  $Zr_5Sn_3$  in systems with such a high zirconium activity (see below),

it drives the disproportionation



through the formation of the very stable ternary solution  $\text{Zr}(\text{Sn},\text{O})$ . For example, the equilibrium product obtained at the approximate limit  $\text{Zr}_4\text{SnO}_{0.17}$  (Table I) would be roughly  $\text{Zr}_{0.885}\text{Sn}_{0.059}\text{O}_{0.056}$  if a limit of 6.2 at. % Sn in the binary is used. This amount of oxygen alone should give the  $\alpha$ -phase at 1050 °C<sup>21</sup> and probably a larger tin concentration if the binary system is any indication. Mixtures of  $\text{Zr}_4\text{Sn}$  and  $\text{Zr}_5\text{Sn}_3$  behave similarly, oxygen always producing some observable amount of  $\text{Zr}(\text{Sn},\text{O})$ , even for the best samples. On the other hand, the effect of oxygen on  $\text{Zr}_4\text{Sn}$  in the binary  $\text{Zr}-\text{Zr}_4\text{Sn}$  region is much less because of the separate zirconium sink, consistent with our diffraction results where only  $\text{Zr}(\text{Sn},\text{O})$  and  $\text{Zr}_4\text{Sn}$  appeared.

We have confirmed the existence of an analogous (A15) lead phase with a composition in the range  $\text{Zr}_{5.5-6.0}\text{Pb}$  and find it to be even more sensitive to decomposition in the presence of oxygen.<sup>19</sup>

A marginal stability of  $\text{Zr}_4\text{Sn}$  has been suggested before,<sup>3</sup> and the apparent sensitivity of  $\text{Zr}_4\text{Sn}$  to the particular impurity oxygen is not without precedent. The addition of even a small amount of iron to the  $\text{Zr}-\text{Sn}$  system does similarly, the  $\text{Zr}_4\text{Sn}$  component disappearing with only 1.0–1.5 at. % Fe at 900–1000 °C.<sup>22</sup> The iron presumably partitions into  $\beta$ -Zr ( $\geq 960$  °C) and  $\text{Zr}_5\text{Sn}_3$  under these circumstances. Regarding the latter, we have seen the formation of the mixed interstitial  $\text{Zr}_5\text{Sn}_3(\text{Sn}_{1/3}\text{Fe}_{1/3})$  derivative of the  $\text{Zr}_5\text{Sn}_3$  host under similar conditions in X-ray and EDX studies of melt-anneal products.<sup>19</sup> More zirconium leads to the formation of the  $\theta$  phase, hexagonal  $\text{Zr}_6\text{Sn}_2\text{Fe}$ , while less tin gives the iron-substituted  $\text{W}_5\text{Si}_3$ -like  $\text{Zr}_5\text{Sn}_{2+x}\text{Fe}_{1-x}$ .<sup>23</sup> Oxygen also shows a remark-

able interstitial binding in  $\text{Zr}_5\text{Sn}_3$  ( $\text{Mn}_5\text{Si}_3$ -type) under conditions where the zirconium activity is lower and  $\text{Zr}(\text{O})$  does not form. The resulting  $\text{Zr}_5\text{Sn}_3\text{O}$  exhibits a significant lattice contraction.<sup>19</sup> A related chemistry is known for the isostructural  $\text{Zr}_5\text{Sb}_3$ .<sup>24</sup>

The lack of deposition of  $\text{Zr}_4\text{Sn}$  from  $\alpha$ -Zr(Sn) and the low-volume fraction of an unidentified (tin-richer) product observed by Carpenter et al.<sup>15</sup> appear to take on a different meaning at this point. A significant effect of oxygen on the  $\alpha$ -Zr(Sn) solidus boundary could be responsible. Although this has never been studied directly, one can infer from the separate  $\alpha$ -Zr(Sn)<sup>3</sup> and  $\alpha$ -Zr(O)<sup>21</sup> boundaries that oxygen probably greatly expands the  $\alpha$ -Zr region. There is some speculation that impurities raise the (apparent) tin solubility.<sup>3,15</sup> A larger tin solubility found in an older study<sup>11</sup> was accompanied by  $c/a$  ratios for the  $\alpha$ -Zr(Sn) phase that are lower than now accepted,<sup>20</sup> a trend that is associated with binary  $\alpha$ -Zr(O) relative to  $\alpha$ -Zr(Sn), as discussed earlier. A recent redetermination of the  $\alpha$ -Zr(Sn)- $\text{Zr}_4\text{Sn}$  solidus,<sup>25</sup> basically agreeing with the original report,<sup>4</sup> also illustrates how the usual experimental methods can raise oxygen values to ~1400, even 3400, ppm atomic. Unfortunately, lattice dimensions were not reported. The absence of  $\text{Zr}_4\text{Sn}$  deposition from the zircalloys in any particular study cannot be clarified until it is ascertained whether an increased partial tin solubility, or a greatly altered temperature dependence of the same, is associated with oxygen, iron, etc., impurities.

**Acknowledgment.** We are indebted to S. C. Sevov for assistance with the SEM-EDX analyses and to H. F. Franzen and his group for use of the arc-melting equipment.

**Registry No.**  $\text{SnZr}_{4.0-4.2}$ , 138008-37-4;  $\text{O}_2$ , 7782-44-7;  $\text{Sn}_3\text{Zr}_5$ , 58799-99-8;  $\text{O},\text{Sn},\text{Zr}$  base, 85088-63-7.

(21) Abriata, J. P.; Garcés, J.; Versaci, R. *Bull. Alloy Phase Diagrams* 1986, 2, 116.

(22) Tanner, L. E.; Levinson, D. W. *Trans. Am. Soc. Met.* 1960, 52, 1115.

(23) Kwon, Y.-U.; Sevov, S. C.; Corbett, J. D. *Chem. Mater.* 1990, 2, 550.

(24) Garcia, E.; Corbett, J. D. *Inorg. Chem.* 1990, 29, 3274.

(25) Arias, D.; Roberti, L. 1982, unpublished research cited in ref 3 (ASM Repository APD-R-83-003).